

$\pi\Lambda\Sigma$ Coupling Extracted from Hyperonic Atoms

B. Loiseau*

*Laboratoire de Physique Nucléaire et de Hautes Énergies[†],
LPTPE, Université P. & M. Curie, 4 Place Jussieu, 75252 Paris Cedex 05, France*

S. Wycech[‡]

Soltan Institute for Nuclear Studies, Hoża 69, PL-00-681, Warsaw, Poland

The latest measurements of the atomic level width in Σ -hyperonic Pb atom offer the most accurate datum in the region of low-energy Σ -hyperon physics. Atomic widths are due to the $\Sigma N - \Lambda N$ conversion which in high angular momentum states is dominated by the one pion exchange. A joint analysis of the $\Sigma^- p \rightarrow \Lambda n$ scattering data and atomic widths allows to extract the pion-hyperon coupling constant $f_{\pi\Lambda\Sigma}^2/4\pi = 0.048 \pm 0.005$ (statistic) ± 0.004 (systematic) or $G_{\pi\Lambda\Sigma}^2 = 13.3 \pm 1.4$ (statistic) ± 1.1 (systematic).

I. INTRODUCTION

It has been known for some time that hadronic atoms allow to test the long range part of hadron-nucleon interactions, the one-pion exchange (OPE), [1,2]. Ideal conditions are found in high angular momentum atomic states. There, the centrifugal barrier prevents the hadron to get close to the nucleus and the OPE effect is strongly enhanced over the effects of two-pion or heavier meson exchanges. Detailed investigations are rather involved. In the best studied cases of antiprotonic atoms most of the long range pionic effects disappear due to spin and isospin averaging over the nuclear states of the bound nucleon. Decays of Σ -hyperonic atoms offer here a better chance, even though the experimental data are in general rather uncertain [3–5]. One exceptional case is the relatively recent measurement of Powers *et al.* [5] that provides a precise width of 17(3) eV for the Σ^- Pb atom in an "upper" $n = 10, l = 9$ state. It gives a good opportunity to study the role of one-pion exchange.

The lifetimes of Σ atoms are determined by the rate of the reaction



occurring at the nuclear surface. This process of hyperon conversion is dominated by the OPE and we exploit this feature to do a best estimate of the $f_{\pi\Lambda\Sigma}^2$ coupling constant. Reaction (1) has been studied in scattering experiments at low energies but the data are sparse and not very precise [6,7]. Differential cross sections are very uncertain. These, as well as the elastic and other inelastic hyperon interactions, have been described by meson-exchange models [8–11]. In addition to OPE, other short-range interactions are found to contribute. On the other hand, in high angular momentum atomic states of Σ atoms, the effects of short-range forces are strongly suppressed. The $\Sigma - N$ interactions in these atomic states are somehow equivalent to interactions in high partial waves of the free $\Sigma - N$ system. However, there is a price for this simplicity: the atomic system involves the rather intricate nuclear structure. The latter determines the initial state of the atom and affects the final decay states. Fortunately, the conversion happens on a proton and the nuclear proton-density distributions are well known from μ atoms and electron scattering data. In addition, the proton momenta are quite well determined by nuclear shell models. The final states of the nucleus, Λ and neutron are less certain, however. These enter into the formalism, essentially in terms of the energy conservation that determines the energy and momentum transferred by the exchanged pion. In this paper it is shown that the atomic-level widths are very stable against these uncertainties.

In section II of this paper we present the formalism and the determination of the $\pi\Lambda\Sigma$ coupling constant from the atomic widths. In addition to the Pb datum, the most accurate older results are also included into the best fit procedure. Some details of the OPE are given in Appendix A while Appendix B discusses the atomic wave functions. In section III limitations and uncertainties of our method are discussed and the error of the extracted $\pi\Lambda\Sigma$ coupling

*Internet address: loiseau@in2p3.fr

[†]Unité de Recherche des Universités Paris 6 et Paris 7, associée au CNRS

[‡]Internet address: wycech@fuw.edu.pl

constant is evaluated. These limitations stem from two sources: first the hyperon conversion process is not described by the pion exchange alone, there exist other amplitudes due to short ranged processes. Several models of these additional amplitudes are used and tested against the scattering data. The effect of such amplitudes on the atomic widths is found to be a 10% correction. The determination of the $\pi\Lambda\Sigma$ coupling is weakly affected. Other uncertainties are due to the nuclear physics involved in the process. All these generate systematic errors which are comparable to the statistical one.

II. THE NUCLEAR CONVERSION OF ATOMIC Σ HYPERONS

The Σ^- hyperon, bound into atomic orbits, cascades down to states where it becomes converted into Λ . The quantum numbers and lifetimes of such states have been determined in X-ray experiments [3], [4], [5]. It turns out that these are levels of high angular momenta which force the conversion process to occur at the nuclear surface. The overlaps of the nuclear and atomic densities are localized in extreme surface regions and extend to distances as large as twice the nuclear radius [12]. Nuclear densities involved in the "upper" levels (states of the highest available angular momenta) amount to 3% of the central density. Processes of such peripherality allow for the standard low density simplifications: quasi-free scattering and single-particle picture of the nucleus. The final states may be described as free states. On the other hand, there exist a difficulty inherent to the surface studies related to the sensitivity to all ranges. For the problem of interest, we turn it into an advantage as it will allow us to precise the $\pi\Lambda\Sigma$ coupling.

This section presents the description of the $\Sigma - \Lambda$ conversion mechanism. It follows the calculation performed in Ref. [13] for the antiprotonic atoms. First, a simple phenomenological picture based on the optical potential model is presented. Next, we elaborate a unitarity relation for reaction (1) and finally some technical details of this calculation are discussed.

The tool to describe the atomic-level shifts and widths due to nuclear interactions is an optical potential, V^{opt} . The simplest one is usually [12] assumed to have the form

$$V^{opt}(\mathbf{R}) = \frac{2\pi}{\mu_{\Sigma N}} \int d\mathbf{u} \rho(\mathbf{R} - \mathbf{u}) t_{\Sigma N}(\mathbf{u}) \quad (2)$$

where $\mu_{\Sigma N}$ is the ΣN reduced mass, $\rho(\mathbf{R})$ is the nuclear density at a radius \mathbf{R} and $t_{\Sigma N}$ is the elastic scattering matrix. In Eq.(2) the finite range in the ΣN interactions induces a folding of the nuclear density ρ over this range. The atomic level widths are given by

$$\begin{aligned} \Gamma/2 &= - \int d\mathbf{R} \text{Im} V^{opt}(\mathbf{R}) |\Psi_{\Sigma}(\mathbf{R})|^2 \\ &= - \frac{2\pi}{\mu_{\Sigma N}} \int d\mathbf{R} \int d\mathbf{u} \rho(\mathbf{R} - \mathbf{u}) \text{Im} t_{\Sigma N}(\mathbf{u}) |\Psi_{\Sigma}(\mathbf{R})|^2 \end{aligned} \quad (3)$$

where $\Psi_{\Sigma}(\mathbf{R})$ is the atomic wave function that involves effects of nuclear interactions. Since $\Psi_{\Sigma} \sim R^l$ and since the angular momenta l are large, the nuclear and atomic densities entering into Eq.(3) are well separated and it is only the longest range components of $\text{Im} t_{\Sigma N}(\mathbf{u})$ that matter. To simplify the discussion we consider the widths of "upper" atomic levels, only. There are three advantages of this choice : i) the most precise data, ii) the largest l and iii) the almost unperturbed hydrogen-like atomic wave functions. The optical potential given by Eq.(2) has some phenomenological success [12] but for the purpose of this study we need a more microscopic approach that discloses the strength and range involved in $\text{Im} t_{\Sigma N}$. This quantity is related by unitarity to the inelastic reactions $\Sigma^- p \rightarrow \Lambda n$, $\Sigma^0 n$. In addition some specific atomic conditions must be met : the initial hyperon and nucleon are bound and then the $\Sigma^0 n$ channel is blocked [1]. The unitarity condition is also affected by the presence of the nucleus. The latter takes away some recoil energy and may induce final state interactions of the outgoing hadrons. These interactions are neglected since the process is an extremely peripheral one, there are no Coulomb interactions and the final particles share about 70 MeV kinetic energy. On the other hand an assessment of the nucleon binding, of the nuclear recoil and of the rearrangement energies is of significance and will be studied below.

A. The atomic-level widths and the unitarity condition

The aim of this section is to calculate the rate of the nuclear $\Sigma - \Lambda$ conversion. This is done in two steps:

1) An amplitude for the $\Sigma p - \Lambda n$ conversion is given in the leading order by OPE. This amplitude is introduced into the nuclear transition matrix element. Other "background" amplitudes, t_b , will be discussed later.

2) The Λ emission probabilities are calculated and summed over states of Λ , n and over states of the final nucleus. For an isolated Σp pair this procedure would produce the inelastic cross section and, via the unitarity condition, the absorptive amplitude $\text{Im } t_{\Sigma N}$. Here, the summation over final states extends over free Λ , n states and over single proton-hole nuclear states. This summation generates $\text{Im } t_{\Sigma N}$ and in the nuclear case it is folded over nuclear and atomic wave functions. These wave functions arise in the form of mixed single particle density matrices.

Assume that the Σ hyperon in an n -th atomic state of quantum numbers $[n, l, m]$ and a proton in a single particle state α convert into a free Λ and a neutron. The transition amplitude for this process is

$$A_{n,\alpha,P,q} = \int d\mathbf{x}d\mathbf{y} \Psi_{\Sigma}(\mathbf{x})\varphi_N^{\alpha}(\mathbf{y}) V_{\pi}(\mathbf{x} - \mathbf{y}) \exp(i\mathbf{P}\cdot\mathbf{R} + i\mathbf{q}\cdot\mathbf{r}) \quad (4)$$

where $\varphi_N^{\alpha}(\mathbf{y})$ are the nuclear wave functions and $V_{\pi}(\mathbf{x} - \mathbf{y})$ is the OPE potential the expression of which is derived in Appendix A. The momenta and coordinates (\mathbf{P}, \mathbf{R}) refer to the center of mass while (\mathbf{q}, \mathbf{r}) denote the relative coordinates for the final pair. The final nucleus is specified, in the spirit of the impulse approximation, to be the initial nucleus left with a hole in the single particle state α .

To calculate the absorption widths, amplitudes $A_{n,\alpha,P,q}$ of Eq.(4) are squared, summed over the final nuclear states and integrated over the phase space of the Λ, n pair. In this way one obtains the following expression for the atomic level widths:

$$\Gamma/2 = \sum_{\alpha} \int d(\mathbf{R}\mathbf{R}'\mathbf{r}\mathbf{r}') d(\mathbf{P}\mathbf{q}) \bar{\Psi}_{\Sigma}(\mathbf{R}' + a\mathbf{r}') \Psi_{\Sigma}(\mathbf{R} + a\mathbf{r}) \bar{\varphi}_N^{\alpha}(\mathbf{R}' - b\mathbf{r}') \varphi_N^{\alpha}(\mathbf{R} - b\mathbf{r}) \\ \times V_{\pi}(\mathbf{r})V_{\pi}(\mathbf{r}') \frac{\mu_{N\Lambda} \pi \delta(Q - E(P) - E(q))}{2\pi(2\pi)^6} \exp(i\mathbf{P}\cdot(\mathbf{R} - \mathbf{R}') + i\mathbf{q}\cdot(\mathbf{r} - \mathbf{r}')). \quad (5)$$

The coefficients $a = M_N/(M_N + M_{\Sigma})$ and $b = M_{\Sigma}/(M_N + M_{\Sigma})$ come from the transformation to the C.M. coordinates. The energy excess $Q = M_{\Sigma} - M_{\Lambda} - E_B(\alpha)$ is due to the hyperon mass difference reduced by the nucleon binding $E_B(\alpha)$. The values of Q fall in the range of 70 – 80 MeV, sizable by the nuclear standards and lead to simplifications that are valid at the nuclear surface. With typical Σ and p momenta that are met in this region one finds the final C.M. recoil energy $E(P)$ to be about 10% of the relative kinetic energy $E(q)$. Hence an average value for this recoil energy is used in Eq.(5). This allows to do the integration over \mathbf{P} which generates a $\delta(\mathbf{R} - \mathbf{R}')$ and brings some simplicity to the otherwise involved integral. The calculations that follow are straightforward although the numerics has to be performed with care.

The energy conservation fixes the final state relative momentum q which is also the momentum carried by the π meson. The actual value of q depends on the nucleon binding and recoil energies. Its central value is about 260 MeV but some 10% changes follow from the distribution of $E_B(\alpha) + E(P)$ which characterizes proton states localized at the extreme nuclear surface. These changes are significant.

B. Range effects

In the limit of zero range ΣN interactions, formula (5) for the conversion width may be expressed in terms of nuclear densities. For finite-range interactions the single-particle wave functions generate mixed densities. However, for simplicity and reference to the experimentally tested charge densities, one wants an expression in terms of the true densities. At the nuclear surface this can be done with a good precision, at least for the absorption rates summed over all nucleon states. The relation that allows it has been obtained in Ref. [14] and reads

$$\sum_{\alpha} \bar{\varphi}_N^{\alpha}(\mathbf{R} - b\mathbf{r}') \varphi_N^{\alpha}(\mathbf{R} - b\mathbf{r}) \approx \rho(\mathbf{R} - b\mathbf{u}) J_{nuc}(\tilde{k} bw) \quad (6)$$

where $\mathbf{w} = \mathbf{r} - \mathbf{r}'$, $\mathbf{u} = (\mathbf{r} + \mathbf{r}')/2$, $\rho(\mathbf{R} - b\mathbf{u})$ is the proton density. The $J_{nuc}(x) = 3j_1(x)/x$ is an analog of Wigner function which describes the proton momentum distribution within the nucleus. The \tilde{k} is an effective local momentum. It is calculable in a shell model and at the nuclear surface it can be related to the proton separation energy [15]. In a similar way we express the angular averaged atomic wave functions $\bar{\Psi}\Psi$ by

$$\frac{1}{2l+1} \sum_m \bar{\Psi}_{\Sigma}(\mathbf{R} + a\mathbf{r}') \Psi_{\Sigma}(\mathbf{R} + a\mathbf{r}) \approx |\Psi_{\Sigma}(\mathbf{R} + a\mathbf{u})|^2 J_{at}(aw), \quad (7)$$

and $J_{at}(aw)$ is obtained by an expansion of the atomic wave functions in terms of $a\mathbf{w}$ (see Appendix B). Collecting all formulas from (5) to (7) one arrives at an expression

$$\Gamma/2 = N_f \frac{(\sqrt{2}f_{\pi NN}f_{\pi\Lambda\Sigma})^2}{(m_\pi^2 4\pi)^2} \frac{\mu_{N\Lambda}}{2\pi} q \left(\frac{1}{3} m_\pi^{*4} + \frac{2}{3} q^{*4} \right) \times \int d\mathbf{R} d\mathbf{u} |\Psi_\Sigma(\mathbf{R} + a\mathbf{u})|^2 \rho(\mathbf{R} - b\mathbf{u}) F_{fold}(u). \quad (8)$$

The function F_{fold} that describes the range of atomic-nuclear folding is given by

$$F_{fold}(u) = \int d\mathbf{w} \frac{d\Omega_q}{4\pi} \frac{\exp(-m^* |\mathbf{u} + \mathbf{w}/2|)}{|\mathbf{u} + \mathbf{w}/2|} \frac{\exp(-m^* |\mathbf{u} - \mathbf{w}/2|)}{|\mathbf{u} - \mathbf{w}/2|} \times \exp(i\mathbf{q}\cdot\mathbf{w}) J_{nuc}(bw) J_{at}(aw). \quad (9)$$

To obtain the result of Eq. (8), few simple manipulations were carried out :

1) As shown in Appendix A, the charged pion exchange involves some energy transfer that modifies the pion mass m_π into m_π^* . The $N_f = 1.02$ factor describes off-shell effects for the bound nucleon. The pion exchange potential of Eq.(A5), corrected for the $\delta(\mathbf{r})$ singularity by Eq.(A6) has been used. The derivative operators are transformed by partial integration to derivatives over the initial and final state wave functions. These derivatives contain one large term due to the final Λn relative momentum \mathbf{q} and smaller contributions due to relative momenta of Σ and p . The large momentum produces a dominant q^4 term in the square bracket of Eq.(8). The effect of the initial momenta is obtained by calculating the derivatives over nuclear densities, atomic densities and correlation functions J_{nuc} (6) and J_{at} (7). To the leading order in u/R , w/R these induce a change of q^2 into,

$$q^{*2} = q^2 + [a(l/R - 1/Bn) + b/(2a_p)f_p]^2 - (\tilde{k}b/5)^2,$$

implemented in Eq.(8). It amounts to a 25% correction, to obtain it we used the atomic wave function of Eq.(B2) and a two parameter Fermi (2pF) nuclear density profile $1/(1 + e)$, where $e = \exp[(c - R)/a_p]$, c is the half density radius and a_p is the surface thickness. In terms of the latter $f_p = e/(1 + e)$. Other corrections due to J_{at} and terms $(u/R)^2$, $(w/R)^2$ are found to be negligible.

2) The spins of initial and intermediate baryons are averaged and summed. These generate the 1/3 and 2/3 weights in the square-bracket term of Eq.(8).

Before performing the numerical calculations of Eq.(9), let us elucidate the range involved in the folding function F_{fold} . For the sake of argument let $J_{nuc} = J_{at} = 1$ for these slowly varying functions. By going to Fourier transforms one obtains:

$$F_{fold}(u) = \frac{16}{\pi} \int d\mathbf{p} \frac{d\Omega_q}{4\pi} \frac{\exp(i2\mathbf{u}\cdot\mathbf{p})}{(m^{*2} + (\mathbf{p} - \mathbf{q})^2) (m'^2 + (\mathbf{p} + \mathbf{q})^2)} \quad (10)$$

where m' should be equal to m^* but we have allowed for a more general situation which is met when several mesons of different masses are exchanged. From Eq.(10) one infers that if $m^* = m'$ the integrand dependence on the (\mathbf{p}, \mathbf{q}) angle is rather moderate. The main bulk of $F_{fold}(u)$ is given by $16\pi \exp(-2u\sqrt{m^{*2} + q^2}) / \sqrt{m^{*2} + q^2}$. Its range is related both to the mass of the exchanged meson and to the momentum transfer, as expected from the uncertainty principle. More detailed calculations indicate some longer range contributions that induce small oscillations for very large u . For $m' > m^*$ formula (10) generates an oscillatory behavior of F_{fold} . This may be seen in the limit of large m' which yields

$$F_{fold} = 16\pi \frac{\sin(2qu)}{2qu} \frac{\exp(-2m^*u)}{m'^2 u}. \quad (11)$$

Rapid oscillations in F_{fold} at large values of u suppress such contributions to the atomic width. The $m' \gg m^*$ terms are due to interferences of the pion exchange amplitude and other amplitudes of shorter ranges in space. These may arise from : exchange of heavier mesons, multiple scattering effects that are supposed to be of ranges shorter than $1/2m_\pi$ and vertex functions as shown in Eq.(A7).

Now, we attempt to describe the atomic level widths with the simple OPE mechanism including the form factor of Eq. (A7). The most precise X-ray measurements of the upper level widths are collected in Table I. These results are reproduced by Eq.(8) with the best fit value $f_{\pi\Lambda\Sigma}^2/4\pi = 0.050(6)$ on the confidence level of $\chi^2_{data} = 2.38/4$. In fact the fitted parameter is $f_{\pi NN}f_{\pi\Lambda\Sigma}$, and to obtain the pion-hyperon coupling an average value of $f_{\pi NN}^2/4\pi = 0.08$ was used. These results were obtained with proton densities extracted from the 2pF charge densities of Fricke et.al [17]. The choice of these densities and the method to obtain the proton densities is discussed in more detail in the next section. The error of $f_{\pi\Lambda\Sigma}$ given above is due to the experimental uncertainties. In addition, there exist uncertainties of the nuclear structure and simplifications in the conversion mechanism which induce systematic errors. To obtain these we analyze the Σp inelastic scattering data and discuss the basic nuclear parameters.

III. RESULTS

The nuclear parameters of importance in this calculation are the energy excess Q and the nuclear recoil energy $E(P)$. The energy excess is determined essentially by the separation energy of the valence protons. The recoil energy is given by the Σp pair momentum distribution, which follows the Fourier transforms of $\Psi_{\Sigma}(\mathbf{x}) \times \varphi_N^{\alpha}(\mathbf{x})$. These functions are localized around a point R_o at the nuclear surface. Thus the Fourier transform is peaked at $P \approx L/R_o$ where L is the angular momentum of the pair with respect to the nucleus. The L is a sum of the atomic and nuclear single particle angular momenta $\mathbf{L} = \mathbf{l}_a + \mathbf{l}_n$. Since $l_a > l_n$ the central value of L is l_a and the most likely momentum is $P = l_a/R_o \sim 1 fm^{-1}$. This estimates the recoil energy to be about 10 MeV. More detailed calculations indicate the spread of the recoil energies of some 5 MeV half-width. As discussed in the previous section an average energy $D = \langle E_B(\alpha) + E(P) \rangle$ is used to determine q , the momentum transferred by the pion, and the range involved in the folding function $F_{fold}(u)$. The shell model generates rather small values for D and $D/E(q) < 0.2$. Nevertheless, uncertainties may arise, due to the way one averages over the binding energies $E_B(\alpha)$ or one calculates the recoil momenta P . These may be reflected in a few percent uncertainty in q . This problem is fortunately removed by a remarkable numerical stability of the atomic level width with respect to changes of D . This effect is related to the form of the pion coupling in Eq.(8). For an increased (decreased) q one finds a decrease (increase) in the atomic-nucleus overlap integral which is perfectly balanced by the increase (decrease) of $q \times (q^{*4})$ in Eq.(8). This property holds on a few percent level for D in the region of 5 to 25 MeV. In this calculation we use an average value of $D[MeV] = E_s + 10$ where E_s is the proton separation energy. Changing D by ± 5 MeV one obtains a change of 0.001 for the best fit $f_{\pi\Lambda\Sigma}^2$. This change is used as a partial estimate of our systematic error.

A. Sensitivity study to short range amplitudes

So far the $\Sigma p - \Lambda n$ conversion has been described by the long range OPE amplitude. The justification of this approximation is the high angular momentum barrier that separates the atomic hyperon and the nuclear proton. An additional finding of the previous section is the suppression of an interference of this pion amplitude with amplitudes related to a shorter spatial extent (see Eq. (11)). A check for these additional "background" amplitudes is possible since the free space conversion cross sections are known. In principle, one needs a full interaction model to do that. However the data on the YN interactions are sparse and the models [8] - [11] differ in their content and their results. Here, we take a phenomenological attitude. A plausible form of the background amplitude, motivated by these theoretical models, is assumed. One or two free parameters are used to describe its magnitude. Next these strength parameters are fitted to reproduce the experimental conversion cross sections. The effect of this "background" amplitude on the atomic level width is calculated and the best fit to both atomic and scattering data is used to extract $f_{\pi\Lambda\Sigma}^2$. Several forms of the background amplitude, t_b are used and the coupling constants obtained in this way are compared and "averaged". Such a procedure allows for an estimate of a systematic error in the coupling constant.

The choice for additional amplitudes is based on several observations :

- (1) On the ground of Lippmann-Schwinger equation one expects the scattering $t(r)$ matrix to be of the form

$$t(\mathbf{r}) = V(\mathbf{r}) + V(\mathbf{r}) \int d\mathbf{r}' G(\mathbf{r} - \mathbf{r}') t(\mathbf{r}') \quad (12)$$

where $t(\mathbf{r}) = t_{\pi}(\mathbf{r}) + t_b(\mathbf{r})$. The second term of this equation is due to multiple scattering effects. The "background" amplitude of interest may be due to the short range part of potential $V(r)$ and/or to the multiple scattering contribution. What is significant is that the range involved in both these terms is expected to be at least shorter than that of the two-pion exchange amplitude.

- (2) The low momentum (140 - 170 MeV/c) inelastic $\Sigma^- p$ cross section of Engelman [6] shows no structure and no enhancement at low energies that would indicate a large scattering length in this system. The K- matrix parameterization for a coupled ΛN , ΣN system in this state indicates the dominance of inelastic processes [8]. However, to be on a safe side, we fit the Massachusetts data [7] taken at higher momenta (200 - 580 MeV/c, 8 data points) to be more independent of the initial state interactions.

We consider several models with different background amplitudes. The results of the best fits to the atomic and scattering data are summarized in Table II and plotted in Fig. 1. The content of these models is as follows:

- A) OPE approximation is used to describe both the atomic widths and the reaction cross sections. These quantities are dominated by the tensor part of OPE. The atomic data by itself favor somewhat stronger $f_{\pi\Lambda\Sigma}^2$ coupling, and this is reflected in a small reduction of the best fit in comparison to the result of the previous chapter . The overall fit is very good, and this leaves very little room for other contributions to the $\Sigma - \Lambda$ conversion.

B) The two pion effects are simulated by Yukawa potential of the $1/(2m_\pi)$ range and f_b^2 coupling. It is supplemented with a form factor of source size parameter $\lambda = 1100$ MeV. This force comes predominantly from a repetition of the tensorial force (see Eq. 12) and contributes mostly to the spin triplet state, so the spin dependence of this potential is chosen to be $(3 + \boldsymbol{\sigma}_N \cdot \boldsymbol{\sigma}_Y)/4$. The effect on the best fit $f_{\pi\Lambda\Sigma}^2$ is minute. Similar results are obtained with an assumption of a tensorial form of this two pion force. The background amplitudes contribute some 10% to the atomic widths. A remark could be added at this point. Here one has a charged particle exchange and one knows in the NN sector that the uncorrelated charged two-pion exchange gives a small contribution, there it is dominated by the ρ . One could expect here a similar situation.

C) A tensor component of the force (A4) is used with a large $m' = m_\rho$ mass of 770 MeV and a coupling f_b^2 .

D) From SU(3) symmetry one expects a strong coupling with K meson as found in Refs. [8,11]. The pseudoscalar exchange potential of the type (A5) is used with form factors $\lambda = 1100$ MeV. Our best fit coupling constant $f_b^2 = \sqrt{2}f_{KN\Sigma} f_{KN\Lambda} = -0.19$ to be compared to the value -0.387 of Ref. [8] and -0.416 of Ref. [11], although a much smaller number -0.030 is obtained in Ref. [9]. However, the "background" constants obtained here are just indicative. The data sample is not large enough for a real determination. These couplings contribute very little to the atomic widths and the corresponding χ^2 minima are quite shallow. The "background" amplitudes are used only to estimate the effects of possible short range forces compared to the basic longest range OPE.

E) The ρ meson exchange amplitude of coupling

$$(\boldsymbol{\sigma} \times \mathbf{q}) \cdot (\boldsymbol{\sigma} \times \mathbf{q}) = \frac{1}{3} (-S_T q^2 + 2\boldsymbol{\sigma}_N \cdot \boldsymbol{\sigma}_Y q^2) \Rightarrow \frac{1}{3} (-S_T q^2 - 2\boldsymbol{\sigma}_N \cdot \boldsymbol{\sigma}_Y m_\rho^2) \quad (13)$$

is used with the mass $m_\rho = 770$ MeV and the cutoff range $\lambda = 1100$ MeV.

F) The $\rho + K$ meson exchange amplitude. This is a three parameter fit but only a marginal improvement has been obtained. Again the background amplitudes contribute about 10% to the dominant OPE. Now $f_K^2 = -0.20$ and $f_\rho^2 = 1.7$.

These results show that the best fit value of $f_{\pi\Lambda\Sigma}^2$ depends rather weakly on the uncertain short range interaction mechanism as can be seen in Fig. 1. There the errors shown for each model correspond to the quadratic sum of the statistical and systematic uncertainties discussed previously. From Table II the systematic error due to the imprecise knowledge of the short range interaction is found to be 0.003.

B. The choice of nuclear densities

Nuclear factors of prime importance are the proton density distributions $\rho(r)$. These are based on muonic atoms and electron scattering data. It is known that these experiments determine precisely R_{ms} -the mean square radii of the charge distribution. However, for the problem of interest one needs higher moments of the proton density distribution, and these are not known very precisely. Since the atomic wave function behaves as r^l one could expect the r^{2l} -th moment to play the dominant role. More realistically, due to the exponential term in the wave function of Eq.(B2) it is the r^{2l-2} -th moment of the density that gives the main contribution. According to Eq.(8) we are interested in the moments of proton distributions folded over a form-factor related to the pion exchange. Let us now discuss the relation of these quantities and the uncertainties involved. To be specific we study the best known nucleus ^{40}Ca .

The relation of bare $\langle r^{2l} \rangle$ and folded $\langle R^{2l} \rangle$ density moments may be obtained via studies of the corresponding Fourier transforms as given in Ref. [16]. For $l = 5$ one obtains

$$\langle R^{10} \rangle = \langle r^{10} \rangle + \frac{55}{3} (\langle r^8 \rangle \langle u^2 \rangle + \langle r^2 \rangle \langle u^8 \rangle) + 66 (\langle r^6 \rangle \langle u^4 \rangle + \langle r^4 \rangle \langle u^6 \rangle) + \langle u^{10} \rangle \quad (14)$$

where $\langle u \rangle$ are the moments of the folding function F_{fold} . Similar relations allow to express the proton density moments $\langle r^{2k} \rangle$ in terms of protonic $\langle u_{pcharge} \rangle$ and nuclear $\langle R_{charge} \rangle$ electromagnetic moments. The charge density moments are calculated from the experimental charge densities taken from the compilations of Refs. [17]. One finds five different densities: two sets of 2pF and three sets of 3 parameter Fermi (3pF) profiles (these 3pF will be defined in the following paragraph). Next, we calculate the average proton density moments generated by those densities. These moments contribute to the folded moment of Eq. (14) with the weights of 1, 0.71, 0.02, 0.33, 0.10 and 0.001 respectively. Thus the highest $\langle r^{10} \rangle$ moment contributes less than half of the whole folded moment. On the basis of these five experimental densities one can also calculate an error (r.m.s deviation) of each proton density moment. Thus the error of $\langle r^8 \rangle$ is 11% while the error of $\langle r^{10} \rangle$ is as large as 29%. A total error of $\langle R^{10} \rangle$ obtained from Eq. (14) becomes 18%. The same analysis done for the folded $\langle R^8 \rangle$ moment yields an error of 7.8%. These large errors offer certain upper limits since the errors of the $\langle r^{2k} \rangle$ are correlated and should not be added independently.

A different procedure to calculate the uncertainty is adopted here: for each experimental charge distribution we calculate a corresponding 3pF density. The parameters of this proton density are fixed to reproduce the lowest $\langle R_{charge}^2 \rangle$, $\langle R_{charge}^4 \rangle$ and $\langle R_{charge}^6 \rangle$ moments. Next the atomic level width is calculated for each folded proton density. The mean square error of the average width obtained in this way amounts to 3.4%, only. With the same procedure we obtain errors of the other atomic level widths: 6.4% in Pb (two 2pF and two Gaussian charge density profiles), 10% in Al (three 2pF profiles) and 11% in Si (two 2pF and two 3pF profiles). The overall uncertainty, weighted by the experimental errors, is estimated to be about 5%. For each nucleus we chose the proton density closest to the average and this density is used for further calculations. It turns out that in each case these are the proton densities based on the experimental charge densities by Fricke et.al [17]. The parameters (c , a_p , w) found for the 3pF $((1 + w(R/c)^2)/(1 + e))$ proton density profiles are: (3.01, 0.493, -0.01) for Al, (3.13, 0.479, 0.016) for Si, (3.69, 0.518, -0.09) for Ca and (6.656, 0.474, -0.01) for Pb.

The Σ hyperon in atomic orbit is affected by the complex optical potential of the nucleus. This changes the atomic wave function in the nuclear region. Two opposite effects contribute: i) the nuclear absorption described by $\text{Im } V^{opt}$ tends to suppress the wave function, ii) the $\text{Re } V^{opt}$ is weakly attractive at large distances and tends to enhance the wave function. Typical optical potential strengths are described by a scattering length b_0 . Phenomenological, best fit values are given in Ref. [12] and the simplest choice is $b_0 = (.25 + i.15)fm$ which characterizes an optical potential with the charge density profile. Solving Schrödinger equation for the level width in Pb one finds that the perturbative calculation underestimates the true width by about 11%. The effect of attraction prevails over the repulsive effect due to absorption. The same exists also within our description of the absorption. However, the effect is smaller since our absorptive pion exchange potential is longer ranged than the real potentials.

To account for the multiple scattering effect we express Eq.(8) as the perturbative result for a folded potential as indicated by Eq.(3). A shift of an argument by $a\mathbf{u}$ is necessary to perform this. Next, such a potential is supplemented by the real optical potential discussed above. The level widths obtained from the Schrödinger equation are larger than the perturbative level widths by 5.8% in Pb, 2.9% in Ca, 3.3% in Si and 3.1% in Al. The net result of this calculation is that the coupling constant $f_{\pi\Lambda\Sigma}^2$ extracted from the widths becomes smaller than the constant extracted in a perturbative way. The difference amounts to 4%. These corrections have been included in the final results given in Table II.

The optical potential correction procedure is not unique as a number of real optical potentials exist in the literature [12]. Different values of b_0 induce an additional 1% uncertainty. This we lump together with the uncertainty due to the charge distribution. Now, the total amounts to a 6% effect.

Thus, nuclear densities induce the main part of our systematic error. The corresponding error of 0.003 arises in the $f_{\pi\Lambda\Sigma}^2$ coupling constant.

The mixed nucleon density matrix of Eq. (6) introduces no serious uncertainties. As the ranges involved are given by $1/(2\sqrt{\mathbf{q}^2 + m^*2})$ one needs this expression for $w < 1.5$ fm. The whole effect of J_{nuc} amounts to a reduction of Γ by less than 5% and the uncertainties in Eq.(6) are negligible.

IV. CONCLUSIONS

It has been shown that the upper level widths in Σ hyperonic atoms present a good source of information on the $f_{\pi\Lambda\Sigma}^2$ coupling constants. The complications due to nuclear physics may be kept under a reasonable control. The experimental uncertainties still present a problem.

Averaging the best fits gives a value of

$$f_{\pi\Lambda\Sigma}^2/4\pi = 0.048 \pm 0.005 \text{ (statistic)} \pm 0.004 \text{ (systematic)} . \quad (15)$$

This corresponds to $G_{\pi\Lambda\Sigma}^2/4\pi = f_{\pi\Lambda\Sigma}^2[(M_\Lambda + M_\Sigma)/m_\pi]^2/4\pi$, i.e.

$$G_{\pi\Lambda\Sigma}^2/4\pi = 13.3 \pm 1.4 \text{ (statistic)} \pm 1.1 \text{ (systematic)} . \quad (16)$$

This result is obtained here from the combined analysis of the atomic widths and the inelastic hyperon scattering cross sections. This result differs from the numbers used, or obtained in the analyzes of the scattering data. In particular : $f_{\pi\Lambda\Sigma}^2/4\pi = 0.041$ has been used by Nijmegen group [8,9] while the Jülich group [11] obtains $f_{\pi\Lambda\Sigma}^2/4\pi = 0.034$ and/or $f_{\pi\Lambda\Sigma}^2/4\pi = 0.028$. It turns out that the atomic data favor larger values of the pion hyperon coupling. Had we used a lower value for the pion-nucleon coupling constant such as that determined by the Nijmegen group [9] viz., 0.075, instead of the classical value [18], 0.080, our $f_{\pi\Lambda\Sigma}^2/4\pi$ would even have been 7% larger.

The errors of this determination, summarized in Table III, consist of four components: i) the statistical error due to the data uncertainties, 0.005, the systematic error due to ii) uncertainties in the proton density distributions, 0.003,

iii) uncertainties of the energy release in the capture process 0.001, iv) the uncertainty due to poor knowledge of the short range hyperon-nucleon interactions estimated to be about 0.003. Altogether, an error of 0.007 is obtained. In order to reduce the large statistical part, both new measurements of the Σ atomic widths and free $\Sigma^- p \rightarrow \Lambda n$ scattering data would be welcome.

We thank D. Vautherin for helpful discussions and S. W. is indebted to J. Dabrowski for useful comments. The authors acknowledge support of IN2P3 /INS collaboration agreement and KBN Grant 2P03B 048 12.

APPENDIX A: PION EXCHANGE FORCES

To make the paper self-contained several useful formulas are collected in this appendix. These concern the pion exchange in the $\Sigma N \rightarrow \Lambda N$ conversion. Due to the $M_\Sigma - M_\Lambda$ mass difference this process involves momentum and also some energy transfer. It makes the exchange force to be longer ranged as compared to the $N - N$ interactions. The Σ^- and p being bound into the nucleus are not on mass-shell Dirac spinors. To derive the OPE potential we shall nevertheless consider them as free on mass-shell spinors. The reduction of the pseudo-vector $\gamma_5 \gamma_\mu \partial^\mu \phi_\pi$ pion-nucleon (πN) and pion-hyperon (πY) couplings leads, in the momentum representation, to

$$V_\pi(\mathbf{q}) = \frac{\sqrt{2} f_{\pi NN}}{m_\pi} V_N \frac{f_{\pi \Lambda \Sigma}}{m_\pi} V_Y \frac{1}{(\mathbf{p}' - \mathbf{p})^2 - (\Delta E)^2 + m_\pi^2} \quad (\text{A1})$$

where

$$V_N = \sqrt{(E_n + M_N)(E_p + M_N)} \boldsymbol{\sigma}_N \cdot \left(\frac{\mathbf{p}'}{E_n + M_N} - \frac{\mathbf{p}}{E_p + M_N} \right) \quad (\text{A2})$$

and

$$V_Y = \frac{M_\Sigma + M_\Lambda}{2} \sqrt{\frac{(E_\Lambda + M_N)(E_\Sigma + M_N)}{M_\Lambda M_\Sigma}} \boldsymbol{\sigma}_Y \cdot \left(\frac{\mathbf{p}'}{E_\Lambda + M_\Lambda} - \frac{\mathbf{p}}{E_\Sigma + M_\Sigma} \right). \quad (\text{A3})$$

Here \mathbf{p} and \mathbf{p}' denotes the initial and final C.M. momenta of the reaction (1), $E_n = \sqrt{\mathbf{p}'^2 + M_N^2}$, $E_p = \sqrt{\mathbf{p}^2 + M_N^2}$, $E_\Lambda = \sqrt{\mathbf{p}'^2 + M_\Lambda^2}$ and $E_\Sigma = \sqrt{\mathbf{p}^2 + M_\Sigma^2}$. In the free space $\Delta E = E_n - E_p = E_\Sigma - E_\Lambda$. If one neglects \mathbf{p}'^2 , \mathbf{p}^2 terms and $\Lambda - \Sigma$ mass difference, Eq. (A1) with Eqs. (A2) and (A3) reduce the corresponding momentum representation OPE to

$$V_\pi(\mathbf{q}) = \frac{f^2}{m_\pi^2} \frac{(\boldsymbol{\sigma}_N \cdot \mathbf{q})(\boldsymbol{\sigma}_Y \cdot \mathbf{q})}{\mathbf{q}^2 - (\Delta E)^2 + m_\pi^2} \quad (\text{A4})$$

where $\mathbf{q} = \mathbf{p}' - \mathbf{p}$ is the momentum transfer. In the atomic state $\Delta E = E_{\Sigma N} - E_{\Lambda N}$ is the energy transferred by mesons. The ΔE of ≈ 40 MeV at low energies makes an effective pion mass $m^* = \sqrt{m_\pi^2 - (\Delta E)^2}$ of about 135 MeV. The coupling constant appropriate for $\Sigma^- p \rightarrow \Lambda p$ reaction is $f^2 = \sqrt{2} f_{\pi NN} f_{\pi \Lambda \Sigma}$. In principle, it is the hyperonic constant $f_{\pi \Lambda \Sigma}$ which is to be determined here. In reality, this determination is affected by a small uncertainty of the pion nucleon constant $f_{\pi NN}$ [18].

In the coordinate representation the potential of Eq.(A4) corresponds to

$$V_\pi(r) = \frac{f^2}{m_\pi^2} (\boldsymbol{\sigma}_N \cdot \boldsymbol{\partial})(\boldsymbol{\sigma}_Y \cdot \boldsymbol{\partial}) \frac{\exp(-m^* r)}{4\pi r}. \quad (\text{A5})$$

This potential is strongly singular at the origin, and this singularity has to be removed by a zero in the wave function induced by a repulsive core potential. A simpler and more customary way is to remove the $\delta(\mathbf{r})$ like term from expression (A5), [19]. This is conveniently done in momentum representation (A4) by the splitting

$$(\boldsymbol{\sigma}_N \cdot \mathbf{q})(\boldsymbol{\sigma}_Y \cdot \mathbf{q}) = \frac{1}{3} (S_T q^2 + \boldsymbol{\sigma}_N \cdot \boldsymbol{\sigma}_Y q^2) \Rightarrow \frac{1}{3} (S_T q^2 - \boldsymbol{\sigma}_N \cdot \boldsymbol{\sigma}_Y m^{*2}) \quad (\text{A6})$$

where $S_T = 3(\boldsymbol{\sigma}_N \cdot \hat{\mathbf{q}})(\boldsymbol{\sigma}_Y \cdot \hat{\mathbf{q}}) - \boldsymbol{\sigma}_N \cdot \boldsymbol{\sigma}_Y$ is the tensor force that does not induce the $\delta(\mathbf{r})$ singularity. The step indicated by arrow in Eq.(A6) describes the subtraction of $\delta(\mathbf{r}) \boldsymbol{\sigma}_N \cdot \boldsymbol{\sigma}_Y f^2/m_\pi^2$ from the spin-spin potential. For the $\Sigma - \Lambda$ conversion one finds $q > 2m^*$ which makes the tensor force to be the strongly dominant one.

The size of pion source is described by a vertex function $F_{\pi BB} = (\lambda^2 - m^{*2})/(\lambda^2 + q^2)$ that induces a change in the pion potential $V_\pi(q) \Rightarrow V_\pi(q)F_{\pi BB}F_{\pi\Lambda\Sigma}$. The same source size parameter $\lambda = 770$ MeV is used for the nucleon and hyperon vertices. These vertex functions induce a change in the spatial form of potential (A5)

$$\frac{\exp(-m^*r)}{r} \Rightarrow \frac{\exp(-m^*r)}{r} - \left(\frac{\lambda^2 - m^{*2}}{2\lambda} + \frac{1}{r} \right) \exp(-\lambda r) \quad (\text{A7})$$

This finite source potential is weaker than the point source one. However, in atomic states of high l the effect of source size is very small as the centrifugal barrier suppresses short distances.

Keeping only first order corrections in the atomic states one has $E_n \simeq M_N + \mathbf{p}'^2/(2M_N)$, $E_p \simeq M_N - E_B$, $E_\Lambda \simeq M_\Lambda + \mathbf{p}'^2/(2M_\Lambda)$ and $E_\Sigma \simeq M_\Sigma$. Eqs. (A2) and (A3) reduce to

$$V_N \Rightarrow \left(1 - \frac{E_B}{4M_N} - \frac{\mathbf{p}'^2}{8M_N} \right) \boldsymbol{\sigma}_N \cdot \mathbf{q}$$

and

$$V_Y \Rightarrow \left(1 + \frac{M_\Sigma - M_\Lambda}{2(M_\Sigma + M_\Lambda)} - \frac{\mathbf{p}'^2}{8M_\Lambda} \right) \boldsymbol{\sigma}_Y \cdot \mathbf{q}$$

It can then be seen that the coupling f^2 of Eq.(A5) is renormalized by

$$N_f = \left(1 + \frac{M_\Sigma - M_\Lambda}{2(M_\Sigma + M_\Lambda)} - \frac{E_B}{4M_N} - \frac{\mathbf{p}'^2}{8M_\Lambda} - \frac{\mathbf{p}'^2}{8M_N} \right) \quad (\text{A8})$$

E_B and \mathbf{p}'^2 take slight different values depending on the nucleus considered but on the average $N_f=1.02$. The $f_{\pi\Lambda\Sigma}$ values quoted in this work have been corrected by this renormalization.

The cross section for $\Sigma^- + p \rightarrow \Lambda + n$ within the Born one pion exchange approximation becomes

$$\frac{d\sigma}{d\Omega} = \frac{q_{\Lambda N}}{q_{\Sigma N}} \left(\frac{2\mu_{\Lambda N} \sqrt{2} f_{\pi NN} f_{\pi\Lambda\Sigma}}{4\pi m_\pi^2} \right)^2 F_{\pi BB}^2 F_{\pi\Lambda\Sigma}^2 \frac{m^{*4}/3 + 2q^4/3}{(m^{*2} + q^2)^2} \quad (\text{A9})$$

where $q_{\Lambda N}(q_{\Sigma N})$ are the final(initial) c.m. momenta.

APPENDIX B: ATOMIC DENSITY MATRIX

The unitarity expression for level widths requires some simple representation of the mixed atomic density

$$\rho_{at}(\mathbf{Z}, \mathbf{z}) = \frac{1}{2l+1} \sum_m \bar{\Psi}(\mathbf{Z} + \mathbf{z}) \Psi(\mathbf{Z} - \mathbf{z}) \quad (\text{B1})$$

In the text we have $\mathbf{Z} = \mathbf{R} + a \mathbf{u}$ and $\mathbf{z} = a \mathbf{w}/2$. The $\rho_{at}(\mathbf{Z}, \mathbf{z})$ is evaluated for small z/Z and the expansion parameter becomes $\epsilon = z^2/Z^2 \approx (b/2)^2 w^2/R^2$. For Pb atom this quantity is very small, $\epsilon < 0.002$, but the atomic wave function change rapidly in space and some care is necessary.

The states of interest are the circular orbits and

$$\Psi_{nlm}(\mathbf{Z}) = N_{nl} Y_{lm}(\hat{Z}) Z^l \exp\left(-\frac{Z}{nB}\right) \quad (\text{B2})$$

where B is the Bohr radius and N_{nl} is a normalization. To perform the expansion let us notice that $(\mathbf{Z} + \mathbf{z}) \cdot (\mathbf{Z} - \mathbf{z}) = Z^2 (1 - \epsilon)$, $|\mathbf{Z} + \mathbf{z}| |\mathbf{Z} - \mathbf{z}| = Z^2 (1 + 2\epsilon - 4\epsilon c^2)^{1/2}$ and

$$\frac{(\mathbf{Z} + \mathbf{z}) \cdot (\mathbf{Z} - \mathbf{z})}{|\mathbf{Z} + \mathbf{z}| |\mathbf{Z} - \mathbf{z}|} = x \sim 1 - 2\epsilon + 2\epsilon c^2$$

where $c = \cos(\hat{Z}\hat{z})$. The most important correction in Eq. (B1) is due to spherical harmonics as the hyperon momenta are predominantly tangential to the nuclear surface. One has

$$\frac{4\pi}{2l+1} \sum Y_{lm}(\widehat{Z+z})Y_{lm}(\widehat{Z-z}) = P_l(x) \approx P_l(1-2\epsilon+2\epsilon c^2) \approx 1-l(l+1)\epsilon(1-c^2) \quad (\text{B3})$$

where we use $P_l'(1) = l(l+1)/2$. The other pieces of atomic wave functions expanded in a similar way produce much smaller corrections. Thus $|\mathbf{Z}+\mathbf{z}|^l|\mathbf{Z}-\mathbf{z}|^l \approx Z^{2l}(1+l\epsilon(1-2c^2))$ and

$$\exp\left(-\frac{|\mathbf{Z}+\mathbf{z}|+|\mathbf{Z}-\mathbf{z}|}{nB}\right) \approx \exp\left(-\frac{-2Z}{nB}\right) \left(1+\frac{\epsilon}{nB}\right).$$

Altogether one obtains

$$\begin{aligned} \rho_{at}(\mathbf{Z}, \mathbf{z}) &\approx \rho_{at}(\mathbf{Z}, 0) P_l(1-2\epsilon+2\epsilon c^2) (1+l\epsilon(1-2c^2)) \left(1+\frac{\epsilon}{nB}\right) \\ &\approx \rho_{at}(\mathbf{Z}, 0) P_l(1-4\epsilon/3) (1+l\epsilon/3) \left(1+\frac{\epsilon}{nB}\right) \end{aligned} \quad (\text{B4})$$

where in the last line an average value of $c^2 = 1/3$ was used. In practice it is only the $P_l(1-4\epsilon/3)$ term that is the important one giving a few percent correction to the atomic density $\rho_{at}(\mathbf{Z}, 0)$.

- [1] *Calculation of nuclear capture rates of Σ^- -hyperonic atoms*, K. Bongart and H. Pilkuhn, Phys. Lett. **76B**, 32 (1978).
- [2] *Strong interaction effects in antiprotonic atoms*, J. F. Haak, A. Lande and F. Iachello, Phys. Lett. **66B**, 16 (1977).
- [3] *Intensity measurements on Σ Hyperonic and Kaonic atoms*, G. Backenstoss, T. Bunaciu, J. Egger, H. Koch, A. Schwitter and L. Tauscher, Zeit. Phys. **A273**, 137 (1975).
- [4] *Measurement of strong interaction effects in Σ atoms*, C. J. Batty, S. F. Biagi, M. Blecher, S. D. Hoath, R. A. J. Riddle, B. L. Roberts, J. D. Davies, G. J. Pyle, G. T. A. Squier and D. M. Asbury, Phys. Lett. **74B**, 27 (1978).
- [5] *Strong interaction effect measurements in sigma hyperonic atoms of W and Pb*, R. J. Powers, M. Eckhouse, P. P. Guss, A. D. Hancock, D. W. Hertzog, D. Joyce, J. R. Kane, W. C. Phillips, W. F. Vulcan, R. E. Welsh, R. J. Whyley, R. G. Winter, E. Austin, G. W. Dodson, J. P. Miller, F. O'Brien, B. L. Roberts, D. R. Tieger, R. B. Sutton, and R. Kunselman, Phys. Rev. C **47**, 1263 (1993).
- [6] *Inelastic Σ^-p interactions at low momenta*, R. Engelman, H. Filthuth, V. Hepp and E. Kluge Phys. Lett. **21**, 586 (1966).
- [7] D. Stephen, Ph. D. Thesis, Univ. of Massachusetts 1970.
- [8] *Soft-core baryon-baryon one-boson-exchange models. II. Hyperon-nucleon potential*, P. M. M. Maessen, Th. A. Rijken and J. J. de Swart, Phys. Rev. C **40**, 2226 (1989).
- [9] *Soft-core baryon-baryon potentials for the complete baryon octet*, V. G. J. Stocks and Th. A. Rijken, Phys. Rev. C **59**, 3009 (1999).
- [10] *Soft-core hyperon-nucleon potentials*, Th. A. Rijken, V. G. J. Stocks and Y. Yamamoto, Phys. Rev. C **59**, 21 (1999).
- [11] *Meson-exchange hyperon-nucleon interactions in the free scattering and nuclear matter*, A. Reuber, K. Holinde and J. Speth, Nucl. Phys. **A570**, 543 (1994).
- [12] *Strong interaction physics from hadronic atoms*, C. J. Batty, E. Friedman and A. Gal, Physics Reports 287, 386 (1997).
- [13] *Antiprotonic studies of nuclear neutron haloes*, S. Wycech, J. Skalski, R. Smolanczuk, J. Dobaczewski and R. J. Rook, Phys. Rev. C **54**, 1884(1996).
- [14] *Density matrix expansion for an effective nuclear Hamiltonian*, J. W. Negele and D. Vautherin, Phys. Rev. C **5**, 1472 (1972); idem, Phys. Rev. C **11**, 1031 (1975).
- [15] *A simple approximation for the nuclear density matrix*, X. Campi and A. Bouyssy, Phys. Lett. **73B**, 263 (1978).
- [16] *Multiple scattering expansion for the level shifts*, W. Stepien Rudzka and S. Wycech, Nukleonika **22**, 929 (1977).
- [17] *Nuclear Charge-Density-Distribution Parameters from Elastic Electron Scattering*, H. de Vries, C. W. De Jager and C. de Vries At. Data Nucl. Data Tab. **36**, 495 (1987), *Nuclear Ground State Charge Radii from Electromagnetic Interactions*, G. Fricke, C. Bernhardt, K. Heilig, L. A. Schaller, L. Schellenberg, E. B. Shera and C. W. De Jager, ibidem **60**,177 (1995).
- [18] *Precise strength of the πNN coupling constant*, T.E.O. Ericson, B. Loiseau, J. Rahm, J. Blomgren and N. Olsson, Nucl. Phys. **A654**, 939c (1999), *Determination of the pion-nucleon coupling constant and scattering lengths*, T.E.O. Ericson, B. Loiseau, A. W. Thomas, hep-ph/0009312.
- [19] *Neutron-proton Charge Exchange*, W.R. Gibbs and B. Loiseau, Phys. Rev. C **50**, 2742 (1994).

TABLE I. Experimental and calculated results for upper level widths, $\Gamma(\text{eV})$, in circular orbits. l is the level angular momentum.

Atom	Ref.	l	$\Gamma_{\text{experiment}}(\text{eV})$	$\Gamma_{\text{calculated}}(\text{eV})$
^{27}Al	[4]	4	0.24(6)	0.21
^{28}Si	[4]	4	0.41(10)	0.51
^{40}Ca	[3]	5	0.41(22)	0.17
^{208}Pb	[5]	9	17(3)	15

TABLE II. Summary of the best fits to the atomic and scattering data.

Model	A(π)	B($\pi + V_1(2\pi)$)	C($\pi + V_T(\rho)$)	D($\pi + K$)	E($\pi + \rho$)	F($\pi + K + \rho$)
atomic χ^2/data	2.42/4	2.42/4	2.33/4	2.31/4	2.43/4	2.28/4
full χ^2/data	5.90/12	5.84/12	5.74/12	5.67/12	5.89/12	5.58/12
f_b^2	0	-0.09	2.4	-0.19	0.4	-0.20 (K); 1.7 (ρ)
$f_{\pi\Lambda\Sigma}^2$	0.047(4)	0.045(4)	0.050(4)	0.051(5)	0.047(5)	0.051(5)

TABLE III. Summary of errors in the determination of $f_{\pi\Lambda\Sigma}^2$.

Source of error	Energy release	Proton density distribution	Background	Statistics
Error	0.001	0.003	0.003	0.005

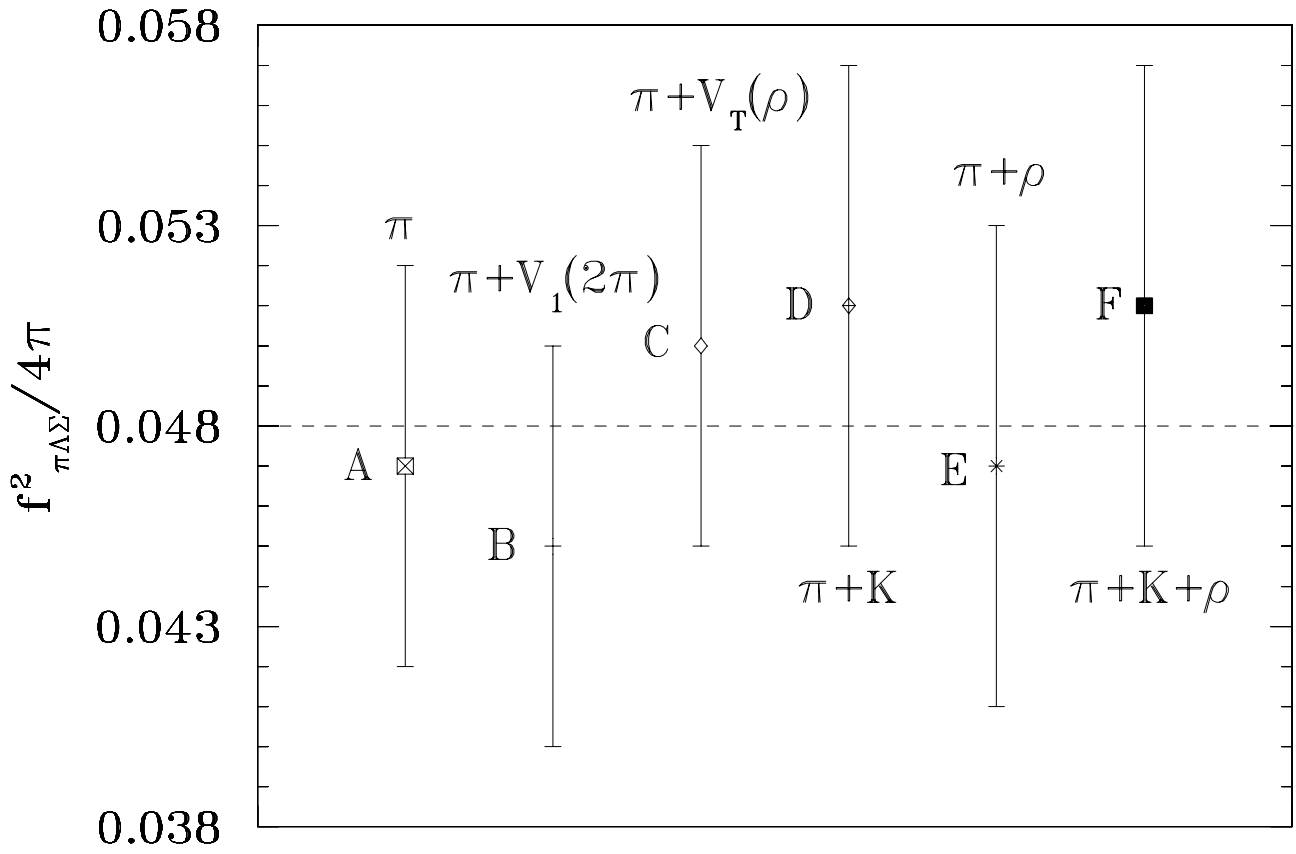


FIG. 1. Results of the best fits to atomic and scattering data with different background amplitudes (see text). Errors are the quadratic sum of statistical and systematic uncertainties